

## **Heat transfer between single cryogen droplet and epoxy skin phantom**

J. Liu<sup>1</sup>, W. Jia<sup>2</sup>, H. Vu<sup>1</sup> and G. Aguilar<sup>1\*</sup>

<sup>1</sup>Department of Mechanical Engineering

University of California-Riverside

Riverside, CA 92507 USA

<sup>2</sup>Beckman Laser Institute

University of California Irvine

Irvine, CA 92615 USA

### Abstract

Cryogen Spray Cooling (CSC) is an auxiliary procedure that pre-cools the epidermis during Laser Dermatologic Surgery (LDS) to avoid non-specific epidermal thermal damage. During CSC, explosive atomization, in-flight evaporation and droplet-substrate interaction affect heat extraction from the substrate. In order to understand the heat transfer mechanism of this complex process, we first study the heat transfer between a single cryogen (R134a) droplet and an epoxy skin phantom. In a high pressure chamber, cryogen droplets are gently deposited on a skin phantom instrumented with a fast-response thin-film thermocouple. The surface temperature variations were recorded and used to calculate surface heat fluxes. Using this setup, we performed experiments to study the effect of initial surface temperature on the cooling efficiency of a cryogen droplet. The results show that the cooling efficiency increases with increasing initial substrate temperature.

---

\*Corresponding author

## 1. Introduction

Laser dermatological surgery (LDS) is the treatment of choice for vascular lesions (e.g., hemangiomas [1] and Port Wine Stain (PWS) [2] birthmarks) as well as aesthetic applications (e.g., hair [3] and tattoo [4] removal). For these conditions, cryogen spray cooling (CSC) is an essential auxiliary method that protects the epidermis from excessive thermal damage during laser irradiation, while the target, such as PWS blood vessels located 100–500  $\mu\text{m}$  below the skin surface [5] are thermally photocoagulated. The only cryogen used for this purpose thus far, approved by the FDA [3], is Tetrafluoroethane-1,1,1,2 (R134a), with a boiling temperature of  $-26^\circ\text{C}$  at atmospheric pressure. Short cryogen spurts (20–100 ms) [6, 7] are released from a pressurized container through a spray valve/nozzle system. Well-atomized cryogen droplets with diameters of 3–20  $\mu\text{m}$  [8] and velocities 10–60 m/s [9] impact onto human skin and extract heat as they spread and evaporate.

Until now, most studies of CSC applied to human skin have assessed the cooling efficiency of a variety of nozzles and/or spraying conditions but assuming or establishing the same initial skin phantom temperature, i.e., room ( $20^\circ\text{C}$ ) or normal skin temperature ( $\sim 30^\circ\text{C}$ ). Recently, however, a new technique consisting of pre-heating skin for a few seconds prior to CSC and laser irradiation was introduced [10]. The ultimate objective of this approach is to elevate sufficiently the temperature of whole skin, including the deep targeted blood vessels, so lower laser energy is required to reach the threshold for damage. For this approach to work, however, it was necessary to prove that the epidermal cooling provided by CSC nozzles could be at least as efficient as with normal initial temperature conditions. Using an aluminum foil sensor it was shown [10] that similar minimal epidermal temperature and thus, higher surface heat fluxes could be reached regardless of the initial skin temperature. A subsequent numerical study [11] suggested that the short period of pre-heating could indeed improve the therapeutic results.

In this study, we aim at providing some insight into the cooling mechanism that dominates the heat extraction process during CSC and provide information for optimization of CSC. For this purpose, we pre-heat a skin phantom (epoxy substrate) to a steady temperature above normal skin temperature. Then we use one single cryogen droplet at room temperature ( $\sim 18^\circ\text{C}$ ), which is gently deposited on a custom-made fast response nickel–copper thin film thermocouple (TFTC) to measure the dynamic temperature variation. Subsequently, we calculate the heat flux between the cryogen droplet and the skin phantom. The results show that pre-heating the skin phantom to 8–

12  $^\circ\text{C}$  above normal skin temperature does not reduce the cooling efficiency of single cryogen droplet.

## 2. Experimental Approaches

To study the heat transfer phenomena between a single cryogen droplet and skin phantom, we conducted our experiments inside a high pressure chamber to control or reduce the evaporation of cryogen at room temperature. Figure 1 shows the schematic of the experimental facilities. Prior to the experiments, the aluminum chamber (11) with acrylic glass windows for imaging and illumination was pressurized to 6.21 bar ( $T_{sat} = 27^\circ\text{C}$ ), which is higher than the saturation pressure of cryogen (R-134a) at room temperature (5.71 bar). A Teflon insulator (1) that holds the heating system (2) and skin phantom with TFTC (4) on top surface is mounted on the translation stage (12) that is used to align the nozzle (5) and TFTC. The cryogen droplets were formed at the tip of small nozzles, which were attached to a needle valve (6) connected to a small cryogen tank (7) pressurized slightly above the chamber's pressure (6.42 bar). The outlet of the nozzle is just 2 mm above the TFTC.

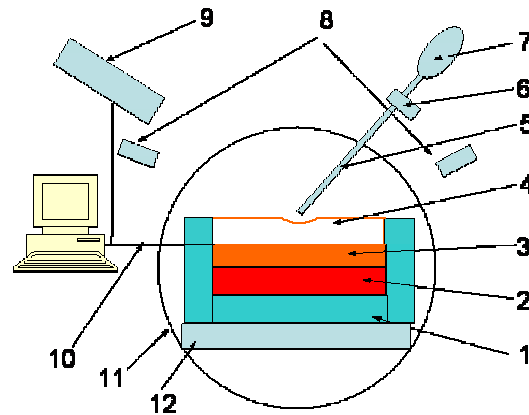


Figure 1. Experimental setup. (1) Teflon insulator, (2) Heater, (3) Heat distributor, (4) Epoxy substrate with TFTC on top surface, (5) Nozzle, (6) Needle valve, (7) Cryogen reservoir, (8) Illuminator, (9) High-speed camera, (10) Data acquisition and control cable, (11) High pressure chamber, and (12) Translation stage.

The skin phantom is made of a mixture of 3100 epoxy resin and A210 Hardener (RBC Industries, Inc., Warwick, RI) with a ratio of 3:1 in weight. The heat conductivity, capacity and density of the epoxy substrate are close to those of the human skin [11]. A spherical-cap shaped indentation (3 mm in depth and 4 mm in radius) that is used to make the cryogen stay on the joint of TFTC was made on the center of the skin phantom. The top surface and the indentation were first polished and cleaned. Thereaf-

ter, the thin-film strips of copper and nickel were deposited sequentially using an E-beam evaporator system (model CV-14, Airco/Temescale). These two strips have a width of 0.5 mm and thickness of 1  $\mu\text{m}$ , respectively and they are overlapped at the center of the indentation, where the droplet is deposited into.

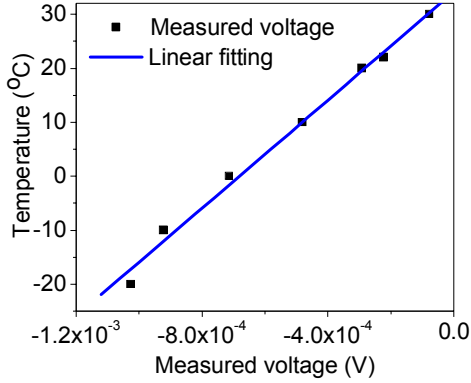


Figure 2. Measured voltages (V) vs. corresponding temperature ( $^{\circ}\text{C}$ ).

Since the TFTC is not a standard thermocouple, we calibrated it by submerging the entire substrate into a liquid bath (model RTE210, Thermo Electron Co.). The temperature of the liquid bath was measured with a K-type thermocouple (model 5TC-KK-(K)-24, OMEGA Engineering, Inc.) and the voltage output of the TFTC was recorded with a data acquisition system (iNet 100, Omega Engineering, Inc.). Figure 2 shows the variation of the voltage output with temperature. As seen, it shows a reasonably good linear relationship for the range of temperatures presented herein ( $-20^{\circ}\text{C}$  to  $30^{\circ}\text{C}$ ), which may be represented by:

$$T(^{\circ}\text{C}) = 49841 \times X(\text{V}) + 34. \quad (1)$$

This TFTC is designed to measure the surface temperature and has two advantages. First, the response time is less than 50  $\mu\text{s}$  [12], therefore it can measure the dynamic temperature change between cryogen and surface. Second, the metal layer is only 1  $\mu\text{m}$  in thickness and with a size of 0.5 mm  $\times$  0.5 mm, thus it creates a minimal disturbance to heat flow across the surface.

Once the surface temperature history is obtained with the TFTC, the heat flux at the surface can then be conveniently obtained using the one-dimensional, semi-infinite medium solution for a step change in surface temperature and applying Duhamel's superposition integral [13, 14].

### 3. Results

Figure 3 shows the measured temperature profiles with different initial skin phantom tempera-

tures. For the four different initial temperatures shown herein, it is seen that the surface temperature drops quickly once the cryogen droplet establishes contact with the skin phantom. Even though the initial substrate temperatures are different, the minimum temperatures measured are similar. For the initial temperatures of  $28.2^{\circ}\text{C}$  and  $31^{\circ}\text{C}$  (normal skin temperature), the temperature variation with time is quite similar and the lowest temperatures reach  $21.2^{\circ}\text{C}$ . For the highest initial temperature ( $39.8^{\circ}\text{C}$ ), the temperature drop rate is the steepest and the minimum temperature that it reaches is  $22^{\circ}\text{C}$ .

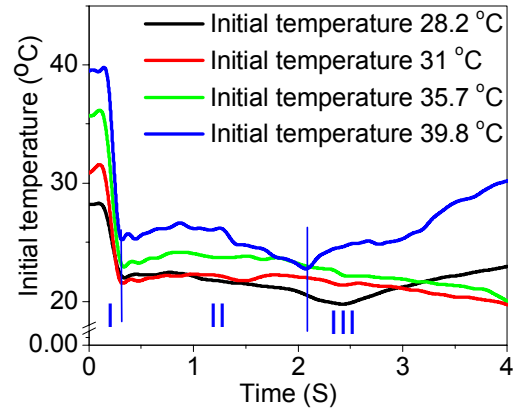


Figure 3. Temperature profile with difference initial surface temperature.

Figure 4 shows the corresponding variation of the heat flux for the four cases presented in Fig. 3. A noticeable increase in the maximum heat flux is appreciated as the initial temperature increases. For the lowest and highest initial temperatures ( $28.2$  and  $39.8^{\circ}\text{C}$ , respectively) the maximum heat fluxes are 7.5 and  $21.2 \text{ kW/m}^2$ , respectively.

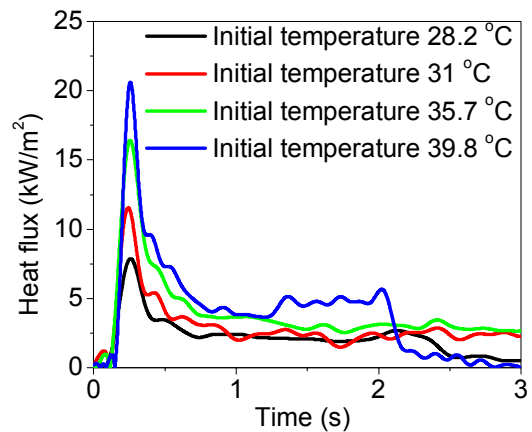


Figure 4. Heat flux profile with difference initial surface temperature.

Figure 5 shows the heat transfer coefficient variation that is calculated according to Fig. 3 and 4. For initial temperature with 28.2°C, the highest value is about 1.6 kW/(m<sup>2</sup>.K), For other three cases, the highest heat transfer coefficients are close at 2.3 kW/(m<sup>2</sup>.K) and almost 40% higher than that of 28.2°C.

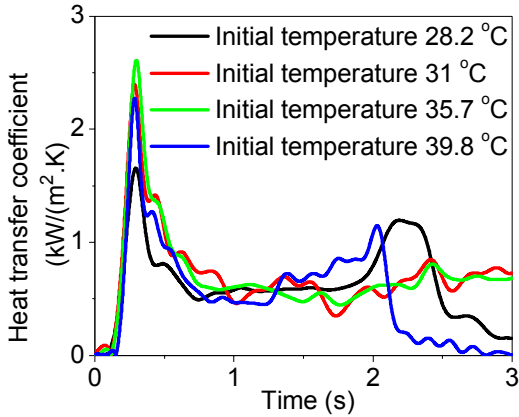


Figure 5. Heat transfer coefficient profile with difference initial surface temperature.

#### 4. Discussion

It is seen that for all four experimental cases, surface temperatures (Fig. 3) drop quickly to  $\sim 22^\circ\text{C}$  from different initial temperature because of the temperature difference with the cryogen droplet deposited at  $18^\circ\text{C}$ . Once the temperature reaches the lowest point, the temperature remains constant for about 3 seconds. After that, the temperature starts to increase slowly as the droplet is completely evaporated.

Both Fig. 3 and 4 suggest that as the initial temperature of the skin phantom increases, the cooling efficiency provided by a single droplet also increases. This is seen, first, in the lowest temperature reached for all four cases, which are very similar and, second, in the maximum heat flux, which is about three times higher for the highest initial temperature ( $39.8^\circ\text{C}$ ) compared to the lowest ( $28.2^\circ\text{C}$ ). That is, while the initial temperature increases by about 33%, the maximum heat flux triples.

These observations are consistent and qualitatively similar to those previously reported by Jia *et al.* [10]. In fact, the same region division of the temperatures measured for CSC by Jia *et al.* [10] may be seen herein in Fig. 3 for the skin phantom with 28.2 and  $39.8^\circ\text{C}$ : Region I, sharp temperature drop due to the CSC droplet contacting with skin phantom; Region II, effective cooling as the deposited cryogen evaporates, and; Region III, temperature increase as the cryogen evaporation is over.

The quantitative differences are worth pointing out too. In the study of CSC [10], the lowest temperature measured was  $-30^\circ\text{C}$  and the total evaporation time less than 200 ms, in contrast to the  $21.2^\circ\text{C}$  and 3 sec of total evaporation time of this study. Furthermore, the measured heat fluxes in Jia *et al.*'s study were all above  $300\text{ kW/m}^2$ , while the highest heat flux reached herein is only  $2.4\text{ kW/m}^2$ . The heat transfer coefficient in Jia *et al.*'s work was at least  $15\text{ kW/(m}^2\cdot\text{K)}$  compared with  $2.5\text{ kW/(m}^2\cdot\text{K)}$  in this study.

These differences may be explained by a combination of factors:

First and perhaps most important is the difference in ambient pressure. In this study, the ambient pressure is controlled just above the saturation pressure, thus the evaporation of the droplet on the surface is slow and heat transfer is dominated by heat conduction and convection. For Jia *et al.*'s work, the heat transfer takes place at ambient pressure, which is  $\sim 6$  bar lower than the saturation pressure of cryogen droplets. Therefore, significant in-flight and on-surface evaporation occur, thus the heat fluxes are much larger and the residual time is much shorter than those measured in this study.

Second, the cryogen droplet is gently deposited on the skin phantom surface, which removes the dynamic effect of impingement, spreading and evaporation of CSC droplets and thus the convective heat transfer. This in fact, represents an excellent method for quantifying the conduction, convective and evaporative effects of droplet CSC.

Finally, in this study the TFTC is built by directly depositing the metal layers on the skin phantom surface. TFTC is only  $1\text{ }\mu\text{m}$  thick, which is much thinner compared to the sensor used on Jia *et al.*'s work, which consisted of an aluminum foil of  $20\text{ }\mu\text{m}$  in thickness. Therefore, the uncertainties in the determination of the surface heat transfer introduced by the TFTC are expected to be even further reduced.

#### 5. Conclusion

Heat transfer between a single droplet and epoxy skin phantom with different initial temperature at elevated ambient pressure was quantified with advanced thin-film thermocouple. The study shows that heat flux and heat transfer coefficient increase with increasing initial skin phantom temperature but the lowest temperature is not affected significantly. As compared to Jia *et al.*'s results, the contribution of heat conduction and convection is not a significant portion of the overall heat flux that takes place during CSC. However, comparisons with CSC heat flux using the TFTC sensor would be more conclusive.

## References

1. Kelly, K.M., et al., *Cryogen spray cooling in combination with nonablative laser treatment of facial rhytides*. Archives of Dermatology, 1999. **135**(6): p. 691-694.
2. Nelson, J.S., et al., *Dynamic epidermal cooling during pulse-laser treatment of port-wine stain-A new methodology with preliminary clinical evaluation*. Archives of Dermatology, 1995. **131**(6): p. 695-700.
3. Goldman, M.P. and R.E. Fitzpatrick, *Cutaneous Laser Surgery*. 1999, Chicago: Mosby.
4. Nelson, J.S., et al., *Selective photothermolysis and removal of cutaneous vasculopathies and tattoos by pulsed laser*. Plastic and Reconstructive Surgery, 1991. **88**(4): p. 723-731.
5. Anvari, B., et al., *Dynamic epidermal cooling in conjunction with laser treatment of port-wine stains: Theoretical and preliminary clinical evaluations*. Laser in Medical Science, 1995. **10**(5): p. 105-112.
6. Aguilar, G., et al., *Influence of nozzle-to-skin distance in cryogen spray cooling for dermatologic laser surgery*. Lasers in Surgery and Medicine, 2001. **28**(2): p. 113-120.
7. Aguilar, G., H. Vu, and J.S. Nelson, *Influence of angle between the nozzle and skin surface on the heat flux and overall heat extraction during cryogen spray cooling*. Physics in Medicine and Biology, 2004. **49**(10): p. N147-N153.
8. Aguilar, G., et al., *Theoretical and experimental analysis of droplet diameter, temperature, and evaporation rate evolution in cryogenic sprays*. International Journal of Heat and Mass Transfer, 2001. **44**(17): p. 3201-3211.
9. Aguilar, G., et al., *Experimental study of cryogen spray properties for application in dermatologic laser surgery*. IEEE Transactions on Biomedical Engineering, 2003. **50**(7): p. 863-869.
10. Jia, W.C., et al., *Heat-transfer dynamics during cryogen spray cooling of substrate at different initial temperatures*. Physics in Medicine and Biology, 2004. **49**(23): p. 5295-5308.
11. Jia, W.C., et al., *Improvement of port wine stain laser therapy by skin preheating prior to cryogen spray cooling: A numerical simulation*. Lasers in Surgery and Medicine, 2006. **38**(2): p. 155-162.
12. Schreck, E., R.E. Fontana, and G.P. Singh, *Thin-Film Thermocouple Sensors for Measurement of Contact Temperatures During Slider Asperity Interaction on Magnetic Recording Disks*. IEEE Transactions on Magnetics, 1992. **28**(5): p. 2548-2550.
13. Taler, J., *Theory of transient experimental techniques for surface heat transfer*. International Journal of Heat and Mass Transfer, 1996. **39**(17): p. 3733-3748.
14. Franco, W., et al., *Radial and temporal variations in surface heat transfer during cryogen spray cooling*. Physics in Medicine and Biology, 2005. **50**(2): p. 387-397.